JOURNAL OF CATALYSIS 97, 390–406 (1986)

An XPS and TPR Study of the Reduction of Promoted Cobalt–Kieselguhr Fischer–Tropsch Catalysts

B. A. SEXTON, A. E. HUGHES, AND T. W. TURNEY

CSIRO Division of Materials Science, University of Melbourne, Parkville, Vic. 3052, Australia

Received March 22, 1985; revised July 28, 1985

Reduction of unpromoted Co- and promoted Co-ThO_2-MgO–Kieselguhr catalysts has been studied with X-ray photoelectron spectroscopy and temperature-programmed reduction techniques. A mechanism of reduction is proposed based on spectroscopic measurements of the surface phases before and after H_2 treatment at 400°C. Cobalt oxide Co_3O_4 is present on all air-calcined catalysts, and is reduced rapidly to CoO at temperatures >300°C in hydrogen. CoO is then more slowly reduced to Co metal on the unpromoted catalysts at 400°C. If the promoters MgO and ThO_2 are present, a reaction between CoO and promoter can occur resulting in new phases which are more resistant to reduction than CoO alone. XPS results suggest one phase as a CoO-MgO solid solution, but the CoO-ThO_2 phase could not be identified. The cobalt in magnesia-promoted CoO phases is reduced completely to the metal at much higher temperatures (500–700°C) but at 400°C the surface reduction is limited to 55% ± 5 after 1 h. Variability in the degree of reduction of various promoted cobalt catalysts is therefore dependent on the nature and loading of the promoter, and the reduction temperature. Promotion of a Co–Kieselguhr catalyst with ThO_2 or MgO does allow a higher degree of control over the CoO reduction kinetics than is found with unpromoted catalysts.

1. INTRODUCTION

The present study was undertaken to characterize the surface phases present on the "classical" Fischer–Tropsch catalyst, Co-ThO_2-MgO–Kieselguhr, under reducing conditions; that is, the precursor states prior to use in the synthesis. In particular, we wished to examine the degree of reduction of cobalt to the metallic phase at the surface, and the effects if any, of the promoters on the reduction process. Although this cobalt catalyst was developed in 1931 (*1*), the mechanism of the promoters' effects during activation and reaction remains mainly speculative, with little published spectroscopic information available. It has been known from the earliest work (*1*) that addition of so-called "structural" promoters MgO and ThO_2 made reduction of cobalt more difficult. Whereas precipitated Co_3O_4 is reduced quantitatively to Co metal at 200–250°C, promoted catalysts, particularly those containing MgO, are only partially reduced for short reduction times at 400°C (*1*). The suggestion has been made by Anderson (*2*) that CoO and MgO may form a solid solution (since they both have the rock-salt structure) and the reduction to cobalt metal is inhibited by a kinetic or thermodynamic effect. We have not been able to find any published spectroscopic work to confirm these hypotheses.

Recent work on XPS surface characterization of cobalt catalysts has concentrated on two main areas: supported-cobalt CO hydrogenation catalysts (*3*, *4*) and Co/Mo/Al_2O_3 hydrodesulfurization catalysts (*5–8*). Castner and Santilli (*3*) recently investigated the reducibility of cobalt on a range of supports. They found that unreactive supports (e.g., SiO_2) initially had a Co_3O_4 phase which reduced completely to metallic Co below 450°C. On more reactive supports (TiO_2, Al_2O_3) interactions between cobalt ions and the support produced surface compound formation which raised the reduction temperature as measured by TPR and XPS. The formation of a "surface spinel" $CoAl_2O_4$ has been well documented in re-

0021-9517/86 $3.00

cent publications (*5, 6*). Cimino *et al.* (*9*) have examined a series of CoO-MgO solid solutions with XPS and found them to be homogeneous with a surface composition similar to the bulk. Hydrogen reduction of Co_3O_4 is known to proceed via CoO to the metal and the possibility of reaction of the active CoO phase with the promoters cannot be ruled out.

In the present work we are concerned only with the catalysts under reducing conditions, and address specifically the degree of reducibility with XPS and TPR. By systematically varying the combinations of cobalt, promoters and support in the TPR and XPS experiments, and by application of curve-fitting techniques in the XPS spectra we present evidence for substantial interaction between promoters and the cobalt species.

2. EXPERIMENTAL

All catalysts were prepared by the method given in example 1 of the patent by Kobylinski (*10*). A mixture of cobalt, magnesium, and thorium nitrates dissolved in 50 ml of hot distilled water [9.88 g $Co(NO_3)_2 \cdot 6H_2O$, 2.20 g $Mg(NO_3)_2 \cdot 6H_2O$, and 0.3 g $Th(NO_3)_4 \cdot 4H_2O$], was precipitated with an excess of hot potassium carbonate solution on BDH acid-washed Kieselguhr (4.0 g), dried at 120°C overnight and finally calcined at 350°C for 16 h. In order to examine the effects of the promoters on the reduction behavior, the following series of catalysts was made: (Co-ThO_2-MgO–KG), (Co-ThO_2–KG), (Co-MgO–KG), (Co–KG), (Co-MgO), and Co_3O_4. The last two samples were precipitated and decomposed in the same way as the other catalysts, omitting the Kieselguhr support. Expressed as a weight ratio, the fully promoted catalyst corresponded to a Co : ThO_2 : MgO : Kieselguhr of 100 : 7 : 17 : 200, which is somewhat higher in magnesia content than the "classical" catalyst described by Anderson (*1*). BET surface areas of the unreduced/calcined catalysts were 95 m^2/g (Co-ThO_2–MgO–KG), 86 m^2/g (Co-MgO–KG), 84 m^2/g (Co-ThO_2–KG), and 56 m^2/g (Co–KG). The Kieselguhr surface area was ~4 m^2/g after acid washing. A Co_3O_4 "model" catalyst was also prepared by air-oxidizing a freshly abraded cobalt high-purity foil (>99.99%) surface at 400°C for 5 min. The film thickness was estimated to be 40 to 50 nm based on the interference color (purple). This model catalyst was used to establish reference binding energies and lineshapes during reduction under conditions of minimal charging, and to study the reduction kinetics of Co_3O_4, in conjunction with Co_3O_4 prepared by precipitation.

Temperature-programmed reductions were carried out in a once-through 5% H_2/N_2 stream at a flow rate of 0.33 ml s^{-1} and a programming rate of 10 K min^{-1}. The sample size was 20 mg with a 60–100 mesh size and the programming range 300–1025 K. For pure Co_3O_4, the sample size was reduced to 6 mg for the TPR runs because the peak shapes were found to be affected by insufficient hydrogen partial pressures when a 20-mg sample was used. The samples were packed in a small quartz tube against a porous plug and immersed in a small programmable tube furnace. No studies of the variation of the H_2/N_2 partial pressure were done although we ensured that the sample size was sufficiently small to be unaffected by diffusion and limiting hydrogen pressure effects. Due to the air sensitivity (pyrophoric nature) of freshly reduced cobalt catalysts, *in situ* reductions were also carried out in a high-pressure flow-through reduction cell in the ESCALAB preparation chamber. The model Co_3O_4/Co foil was reduced at 300°C to study the reduction kinetics and the other catalysts were dispersed as a thin film on nickel plated copper holders and reduced at 300°C (Co_3O_4 only) or 400°C for 1 h (flowing H_2, 15 ml/min at 1 atm). The catalyst powder was normally crushed with a mortar and pestle and dispersed on the surface of the metal holder with an inert hydrocarbon solvent. After drying, the powder layer was outgassed and transferred directly into the

UHV analysis section. We did not use pressed disks, since pressing can introduce surface contamination from the die. Following the reductions, samples were transferred directly into the UHV environment of the ESCALAB analysis chamber, without air exposure, for surface analyses.

XPS analyses were conducted in a V.G. ESCALAB photoelectron spectrometer with Al$K\alpha$ radiation (150 W) at a pass energy of 30 eV (4-mm slits). Signal averaging techniques were used to accumulate the spectra. Scans of the Co 2*p*, O 1*s*, Si 2*s*, Mg 1*s*, and Th 4*f* regions were taken. Charge referencing was accomplished via gold evaporation with the reference line Au $4f_{7/2}$ at 84.0 eV. Quantitative measures of the elemental atomic ratios were calculated from the Scofield cross sections (*11*) and measured intensities, assuming the mean free path ($\alpha E_k^{0.5}$) and transmission function ($\alpha E_k^{-0.5}$) terms cancel. We have found this method to be accurate to $\pm 10\%$ when tested on suitable standards.

Curve-fitting techniques were applied to the O 1*s* region of the catalyst spectra, to separate the contributions from the various oxide phases. We used a peak shape which was the product of a Gaussian and a Lorentzian and had an exponential tail added to the high binding energy side (*12*). The O 1*s* lineshapes for the individual oxide phases were analyzed first to determine fitting parameters before they were incorporated into a full minimization routine. A nonlinear background (*13*) was subtracted from the spectra before any minimization was attempted. The computer program was a quasi-Newton algorithm (Numerical Algorithm Group MK-8, library routine E04JAF) executed on a Cyber 70 Model 76 computer.

Calibration of the reference O 1*s* line positions via gold evaporation for the individual oxide or hydroxide phases was made with reference to the compounds Co_3O_4, CoO, $Co(OH)_2$, ThO_2, MgO, $Mg(OH)_2$, and SiO_2 (from KG). The O 1*s* line positions for Co_3O_4, CoO, ThO_2, and MgO were all within the window 529.5–530.5 eV. $Co(OH)_2$ and $Mg(OH)_2$ both had a line position within the range 531.3 ± 0.5 eV and SiO_2 occurred at 533.0 ± 0.5 eV. The oxygen 1*s* component from ThO_2 was calculated from the Th $4f_{7/2}$ intensity, assuming ThO_2 stoichiometry and added to the spectrum, since it could not be separated in the fitting routine from the Co-O and Mg-O contributions. This was always a minor contribution to the total spectrum, however. MgO was an unusual reference phase in that it tended to hydroxylate readily on exposure to air after calcination. We found that the O 1*s* line from MgO prepared by calcination of the precipitated carbonate at 350°C always occurred at 531.0 ± 0.3 eV in the reference phases MgO, MgO-Co_3O_4, and MgO–KG. Based on this line position, and the peak shape, we concluded that, all of these phases had a high degree of surface hydroxylation of the magnesium-oxygen component, even after calcination at 350°C in air. For the Co-MgO–KG and Co-ThO_2-MgO–KG catalysts, there was an overlap between the Co-OH and Mg-OH components at 531.0 ± 0.3 eV. However, based on the observed tendency for the Mg-O component to be predominantly hydroxylated in the reference phases prepared by the same method, we assign most of the 531.0-eV band to a Mg-OH component. This assignment is supported by the calculation of the expected O 1*s* intensity for the magnesium-oxygen component from the measured Mg 1*s* intensity. For both catalysts we calculated a minimal contribution to the Mg-OH line from additional Co-OH intensity (10–20% maximum).

For all of the spectra, either a two- or three-peak fit was obtained, within the windows defined by the known reference compounds. We checked for other possible solutions (four peaks, e.g.) but were unable to obtain satisfactory fits. In the reduced-catalyst spectra, no significant contributions from hydroxyl line positions near 531.0 eV were obtained. The binding energies (B.E.) measured for CoO (529.5 eV), hydroxyl-

free MgO (530.0 eV), and the CoO-MgO solid solutions (9) (530.0 ± 0.3 eV) were all very similar and no separation of these three phases was obtained.

3. RESULTS

3.1. *Reduction of* Co_3O_4

In this section we examine the reduction of a Co_3O_4 phase both unsupported and supported on cobalt foil to establish reference binding energies and peak shapes and to study the rate of reduction to cobalt metal. The use of the model foil catalyst eliminated charging effects and all B.E.'s were measured directly with respect to the Fermi level. Some charging was observed on the Co_3O_4 powder, and the spectra were consequently broader. The reduction kinetics of the two phases were identical as measured by XPS intensities and binding energies, however. Co_3O_4 (both foil and powder) was analyzed prior to and during reduction at 300°C and 1 atm flowing H_2 in the ESCALAB isolation cell. After reduction for a specific time the samples were cooled in H_2 and transferred to the UHV analysis chamber without air exposure. The XPS results for the Co $2p_{3/2}$ and O 1*s* regions are shown in Figs. 1 and 2, respectively, for the foil-supported oxide.

The calcined surfaces consisted of a slightly nonstoichiometric form of Co_3O_4 as indicated by the Co(III) line at 779.5 eV (no shake-up satellites), the O 1*s* line at 529.4 eV and a calculated O/Co ratio of 1.5 ± 0.1

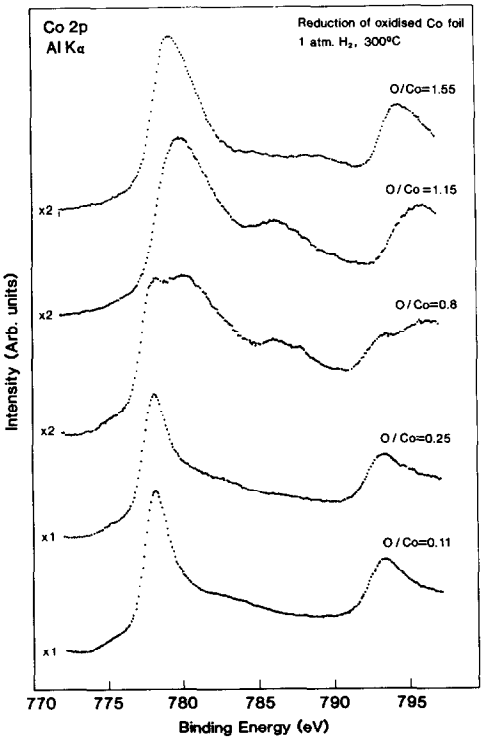

FIG. 1. Co $2p_{3/2}$ spectra for an oxidized cobalt foil (50 nm thickness of oxide) at various O/Co ratios (determined by XPS) during reduction in flowing hydrogen at 300°C. Similar results were observed for Co_3O_4 or Co_3O_4–KG catalysts, with some spectral broadening due to charging. O/Co ratios were calculated from XPS peak areas and cross sections. The air-oxidized film is nonstoichiometric at the surface, exhibiting a slight oxygen excess over the expected Co_3O_4 stoichiometry. Reduction proceeds via CoO to the metal.

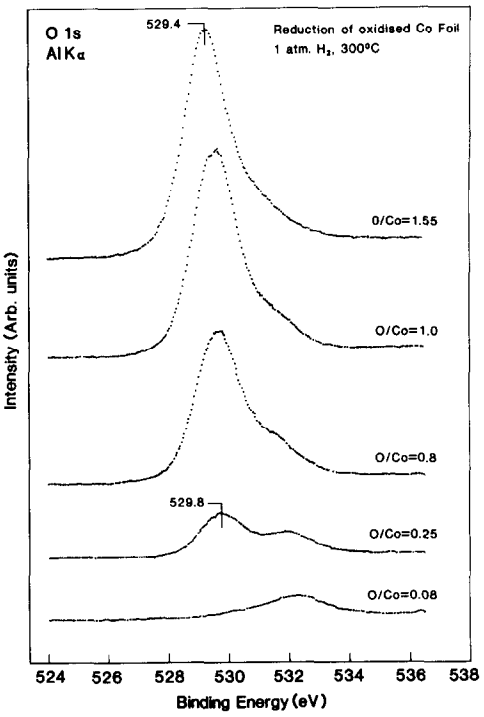

FIG. 2. Oxygen 1*s* spectra for an oxidized cobalt foil at various O/Co ratios during reduction in flowing hydrogen at 300°C. The small peak at 531.5 to 532 eV is attributed to $Co(OH)_2$ formed during the initial low-temperature oxidation. A chemical shift of the O 1*s* from 529.4 to approx. 530.0 eV is observed as the reduction nears completion.

(1.33 theoretical). Brundle (*14*) has previously observed nonstoichiometric oxygen at the surface of Co_3O_4. The excess oxygen uptake creates cation vacancies and oxidizes Co(II) to Co(III). The absence of any substantial shake-up satellite indicates almost entirely Co(III) in the outer Co_3O_4 layers. X-Ray diffraction measurements of the Co_3O_4 sample indicated that Co_3O_4 was the only phase present, hence the nonstoichiometry must be confined to the surface layers. The identical surface stoichiometry and surface spectra for the powder and oxidized foil surfaces is strong evidence that the Co_3O_4 phase is also present on the latter.

During reduction at 300°C the O/Co ratio smoothly decreased and changes occurred in the Co $2p_{3/2}$ region and in the O 1*s* region. Near an O/Co ratio of 1.0 the Co $2p_{3/2}$ B.E. increased to 780.3 eV and the shake-up satellite at ~786 eV intensified. This spectrum is characteristic of Co(II) and in good agreement with Brundle's analysis of CoO (*14*). The O 1*s* B.E. increased slightly to 529.5 eV, but is essentially the same as Co_3O_4. At this point, examination of the reduced oxide powder under vacuum indicated an olive greenish-brown color which is normally associate with bulk CoO. Combined with the O/Co stoichiometry and the presence of Co(II) in the surface spectrum, we believe that bulk reduction to CoO has occurred. With further reduction the O 1*s* peak decreased uniformly in intensity and shifted slightly higher to 529.8–530.0 eV. In the Co $2p_{3/2}$ spectrum the metal line at 778.0 eV appeared with the Co(II) line at 780.3 eV and its satellite decayed in intensity at the expense of the metal. In the O 1*s* region on the foil surfaces we observed a small peak near 531.5–532 eV which is attributed to $Co(OH)_2$ (*15*), formed in air during the initial oxidation. Brundle (*15*) has described preferential growth of $Co(OH)_2$ on foils by low-temperature oxidation in moist air, whereas Co_3O_4 was formed with high-temperature oxidation. Co_3O_4, therefore, is reduced in the sequence $Co_3O_4 \rightarrow CoO \rightarrow Co$

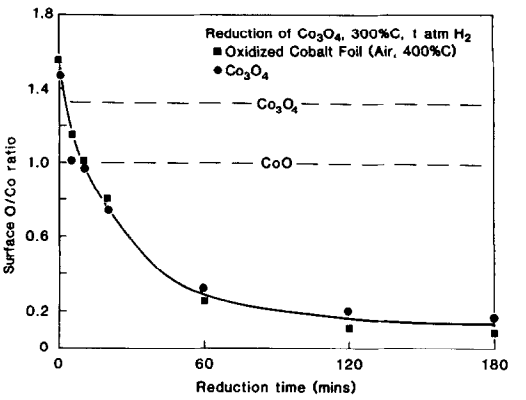

FIG. 3. The atomic O/Co ratio for the air-grown Co_3O_4 film and Co_3O_4 powder as a function of reduction time at 300°C in flowing hydrogen. Similar reduction kinetics are observed for both phases, with almost quantitative reduction to cobalt metal after 2–3 h. O/Co ratios are determined by integration of the XPS peak areas.

with almost quantitative reduction after 3 h at 300°C.

A plot of the O/Co ratio determined by XPS as a function of time during the 300°C reduction is shown in Fig. 3, for both the foil-supported oxide, and the bulk oxide. From the initial O/Co ratio of 1.5 ± 0.1 reduction proceeded rapidly in the first 5 min to the CoO phase. Over the next 2 h, CoO was reduced to metallic cobalt. These results establish that Co_3O_4 heated to 400°C in air has a certain degree of surface nonstoichiometry, and is almost quantitatively reduced to cobalt metal at 300°C in hydrogen. The rapid reduction of Co_3O_4 to CoO is contrasted with the much slower conversion of CoO to the metal and suggests different activation energies for the two processes. This hypothesis is supported by the TPR results in the next section.

During reduction of Co_3O_4, the black initial phase changed to an olive-greenish brown CoO phase (identified from the Co(II) present, and an O/Co ratio close to 1.0) very rapidly then this slowly turned black again as cobalt metal formed. The black-olive green-black sequence was not observed on the foil because the surface film was too thin. XPS results demon-

strated that exposure of either the metal foil or reduced Co_3O_4 powder to air produced rapid oxidation to the oxide CoO which was also unstable and further rapidly oxidized to Co_3O_4 at the surface. The heat of oxidation of cobalt is large enough to cause a pyrophoric effect when the reduced catalysts are exposed to air. This pyrophoric tendency is a major problem in attempting to analyze bulk phases via electron microscopy or XRD since anaerobic facilities are not generally available with these techniques. In Table 1 is a summary of the reference binding energies for Co_3O_4, CoO, Co, and $Co(OH)_2$, determined from the experiments.

3.2. *Temperature-Programmed Reduction of Catalysts*

Figure 4 shows the TPR profiles of the following catalysts; Co-ThO_2-MgO–Kieselguhr, Co-MgO–Kieselguhr, Co-ThO_2–Kieselguhr, Co–Kieselguhr, Co-MgO, Co_3O_4, and β-$Co(OH)_2$. The $Co(OH)_2$ was prepared by precipitation from a cobalt nitrate solution with potassium hydroxide. The TPR profiles for all samples except $Co(OH)_2$ can be divided up into two distinct temperature regimes: regime I, where a narrow peak occurs in the range 250–300°C, and regime II, where a second, broader peak occurs, covering the range 300–700°C. Table 2 gives the quantitative calculation of the percentage reduction to metallic cobalt for (a) regime I and (b) the total area, including both peaks, based on the equation

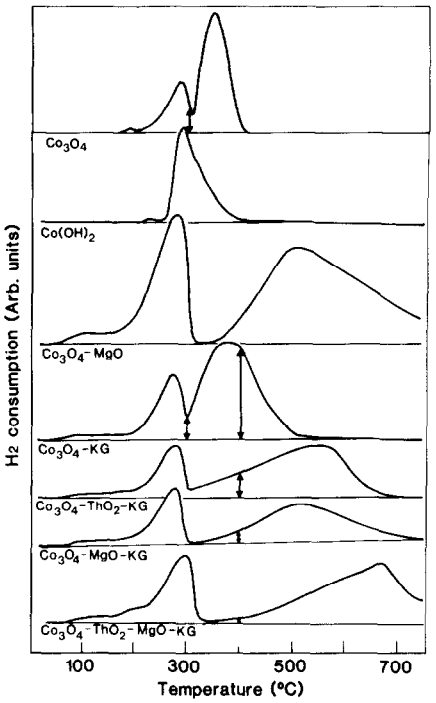

FIG. 4. Temperature-programmed reduction of cobalt catalysts with various compositions (10°C/min programming rate, 5% H_2/N_2 mixture). The two main features are the low-temperature peak below 300°C and the high-temperature peak from 300 to 700°C. The height of the vertical bars above the baseline at 300 and 400°C indicate the relative rates of reduction at these temperatures. These rates are used to explain qualitative differences between the extent of reduction for different catalysts at these temperatures (see text).

TABLE 1

Binding Energies[a] (Al$K\alpha$) of Cobalt Reference Phases

Phase	Co $2p_{3/2}$ (eV)	O 1s (eV)	Comments
Co_3O_4	779.5 ± 0.2	529.5 ± 0.2	Primarily Co(III) at surface.[b] No shake-up satellites
CoO	780.3	529.5	Co(II). Strong shake-up satellites
$Co(OH)_2$	781.1	531.3	Co(II). Strong shake-up satellites
Co	778.0	—	No shake-up satellites

[a] Determined from electrically conducting thin films supported on a high-purity Co foil. Measured w.r.t. Fermi level with a reference B.E. of Au $4f_{7/2}$ 84.0 ± 0.1 eV.

[b] XPS spectra indicated air-calcined Co_3O_4 was slightly nonstoichiometric at the surface, as evidenced by a higher O/Co ratio than expected, and no Co(II) present in the spectrum. The O/Co ratio of 1.5 at the surface indicated a surface composition of Co_2O_3. The stoichiometry is only confined to the surface, however since XRD measurements confirmed the presence of bulk Co_3O_4.

TABLE 2

Percentage Reduction of Catalysts Determined from Temperature-Programmed Reduction[a]

Catalyst (KG = Kieselguhr)	First low-temperature peak[b] (%)	Total reduction (%)
Co_3O_4	25	92
Co_3O_4-MgO	23	99
Co–KG	23	109
Co-ThO_2–KG	25	111
Co-MgO–KG	24	98
Co-ThO_2-MgO–KG	28	100

[a] Based on the equation $Co_3O_4 + 4H_2 \rightarrow 3Co + 4H_2O$.

[b] Expressed as a percentage of the total area under the TPR curve.

$$Co_3O_4 + 4H_2 \rightarrow 3Co + 4H_2O$$

The results in Table 2 show a remarkably constant value of 25 ± 2% for the reduction in the first peak, with 75% in the second. By 700°C, all of the catalysts are completely reduced to the metal. The data in Table 2 are consistent with the following mechanism:

$$\text{Stage I} \quad Co_3O_4 + H_2 \rightarrow 3CoO + H_2O$$
$$\text{Stage II} \quad 3CoO + 3H_2 \rightarrow 3Co + 3H_2O$$

A 25% reduction average for the low-temperature peak is in good agreement with the initial reduction of Co_3O_4 to CoO. The temperature independence of this peak with the method of preparation or the presence of promoters indicates very little, if any, interaction between the Co_3O_4 phase on the catalysts and any of the promoters. In addition, the nonstoichiometry of Co_3O_4 observed in the previous section must be restricted to the surface layers since the hydrogen uptake is close to the theoretical value (implying that the bulk of the oxide has Co_3O_4 stoichiometry). The second peak in the TPR curves must correspond to reduction of CoO, or phases containing the stoichiometry Co : O = 1, to the metal. As distinct from Co_3O_4, the peak maximum and breadth depended markedly on the presence of promoters.

In Fig. 4, the presence of the promoters increases the peak maximum temperatures for Co_3O_4 and Co–KG from below 400°C to 500–680°C. That Kieselguhr has little effect on this second stage of reduction can be seen in comparing the Co_3O_4-MgO catalyst and Co-MgO–KG, both of which have similar profiles. In general, the promoters appear to retard the reduction of CoO, as evidenced by the higher peak reduction temperatures. Of more relevance, however, are the actual rates of reduction, which are indicated by the vertical bars at 300°C (for Co_3O_4 and Co–KG) and 400°C (supported catalysts). The height of the bar above the baseline is proportional to the rate of reduction at that temperature. At 300°C, the reduction has passed the first peak on all catalysts, therefore the reduction of Co_3O_4 to CoO would be rapid at this, and higher temperatures. For Co_3O_4 and Co–KG, however, the rate for the Stage II process is quite substantial (~20% of max. rate) at 300°C, and the Stage II reduction to cobalt metal would be expected to proceed at 300°C, despite being below the peak maximum. In a similar fashion it can be seen that the relative rates of reduction at 400°C are higher for the non-magnesia-containing catalysts, than the magnesia-containing ones, with the order in a different sequence to the peak maxima. We cannot predict what the total reduction will be after a finite time from the TPR, but they can be done via direct measurements of the surface cobalt with XPS (or from total hydrogen uptake measurements).

3.3. XPS

XPS was used to study both (a) the chemical shifts and peak changes induced by reduction and (b) quantitative precipitate: Kieselguhr intensity ratios. A representative spectrum of the fully promoted catalyst Co-ThO_2-MgO–KG is shown in Fig. 5, with the Mg 1*s*, Co $2p_{3/2}$, O 1*s*, Si 2*s*, and Th $4f_{7/2}$ region shown. For the as-prepared catalyst

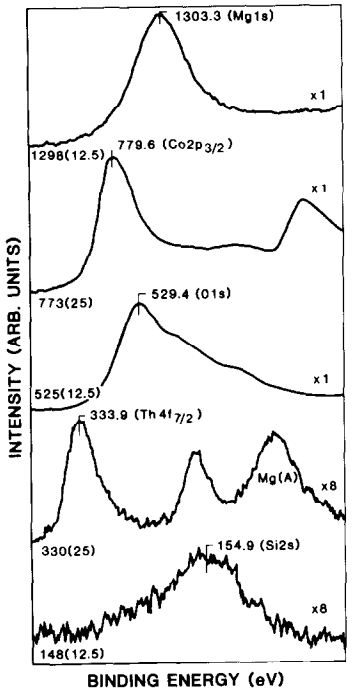

FIG. 5. Representative XPS spectra of a Co-ThO_2-MgO–Kieselguhr catalyst (Al$k\alpha$) in the unreduced (calcined) state. Data are shown for Mg 1*s*, Co $2p_{3/2}$, O 1*s*,Si 2*s*, and Th $4f_{7/2}$ regions. This catalyst was electrically conducting and exhibited no charging.

in Fig. 5, all of the Mg, Th, Si, and Co components were visible with the O 1*s* region showing a complex multiplet due to the overlapping oxide components. The Co $2p_{3/2}$ line had an identical B.E. (779.6 eV) and shape (no shake-up satellite) to the Co_3O_4 film studied previously. The large O 1*s* component at 529.4 eV corresponds to the Co_3O_4 phase, in agreement with the foil results. Both Mg 1*s* (1303.3 eV) and Th $4f_{7/2}$ (333.9 eV) binding energies were similar to MgO prepared by precipitation of the carbonate and ThO_2. After reduction, the Co 2*p* and O 1*s* spectra were substantially changed whereas the Mg 1*s* and Th 4*f* lines indicated no reduction below Mg^{2+} or Th^{4+}. Similar results were found on the singly, or unpromoted catalysts. We therefore analyzed the O 1*s* and Co 2*p* regions in detail, to determine the extent of reduction of the cobalt.

Each catalyst was subjected to a 1-h reduction at 400°C; a temperature sufficient to "activate" the classical catalyst. The Co $2p_{3/2}$ spectra showed that metallic cobalt was formed to different extents on the four catalysts. The results are shown in Fig. 6, with the percentage reduction to the metal listed in Table 3. Owing to the line broadening from charging, we used difference spectra to subtract the metallic contribution from the total envelope to reveal the unreduced Co(II). In determining the percentage reduction in Fig. 6, we took the total cobalt envelope for the reduced catalysts, and fitted a metallic cobalt line (measured from reduced Co_3O_4) to the spectrum, subtracting this component to obtain the unreduced Co(II) component. The criterion for the fit was preservation of the correct lineshape for Co(II). Both Co–KG and Co-ThO_2–KG exhibited similar values of 90 ± 5% reduction after 1 h at 400°C. The magne-

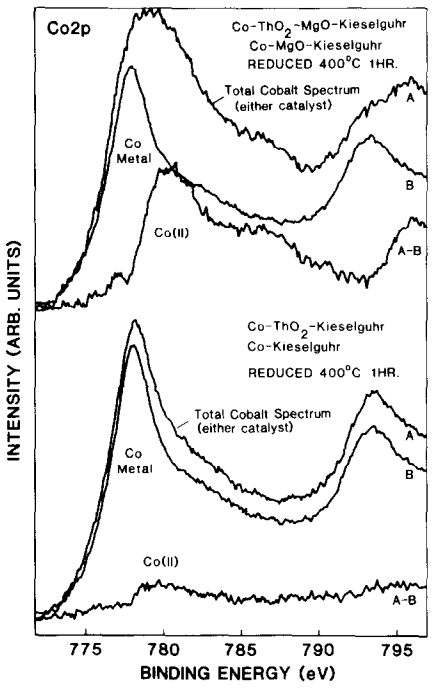

FIG. 6. Difference Co $2p_{3/2}$ spectra for magnesia-promoted and other cobalt catalysts after reduction at 400°C for 1 h in H_2. The cobalt metal lineshape (B) was deconvoluted from the total spectrum (A) to give the residual Co(II) unreduced component (A-B).

TABLE 3

Percentage Cobalt Reduction[a] Derived from the Co $2p_{3/2}$ Peaks

Catalyst	% Cobalt reduction (400°C, 1 h, H_2 flow 1 atm)
Co-ThO_2-MgO-KG	55 ± 5
Co-MgO-KG	55 ± 5
Co-ThO_2-KG	90 ± 5
Co-KG	90 ± 5

[a] Based on the relative areas of the Co (metal) $2p_{3/2}$ peak at 778 eV and the Co(II) peak at 780.3 eV derived from a subtraction procedure (see text). This reduction estimate is for the surface species only, and may differ from the total bulk reduction, if the dispersion of the cobalt metal is different from the other unreduced cobalt phases.

sia-promoted catalysts, both limited at 55 ± 5% reduction to the metal, however. These latter catalysts have a substantial amount of unreduced cobalt in the form of Co(II), as seen in Fig. 6. These ESCA reduction experiments are in qualitative agreement with the TPR rates measured previously, with magnesia containing catalysts having lower reduction rates at 400°C. The surface reduction measured here, however does not necessarily reflect the total bulk reduction since the dispersion of the cobalt metal particles and unreduced Co(II) may be different. In order to obtain some more information concerning the nature of the unreduced Co(II) phases, we examined in detail, the oxygen 1*s* spectra for the series of promoted and unpromoted catalysts.

Data for the O 1*s* regions of the unreduced and reduced catalysts are shown in Figs. 7–10. Line positions for Co-O, Co-OH, Mg-O, Mg-OH, and Si-O were taken from the reference oxides and hydroxides and were allowed to vary within a 1-eV window for the fitting procedure. The O 1*s* line for Th-O overlapped with Co-O and is shown coincident with the Co-O component, calculated from the Th $4f_{7/2}$ intensity (assuming ThO_2). For the Co–KG case (Fig. 7), three components were observed in the unreduced catalyst assigned to Co-O, Co-OH, and Si-O (broadened due to the presence of some surface hydroxyl groups). The presence of a surface hydroxyl component on this catalyst was surprising since much lower hydroxyl levels were observed on unsupported Co_3O_4 alone. The presence of these hydroxyls did not appear to influence the reduction, since both Co-O and Co-OH attenuated dramatically after reduction with only a small Co-O line left near 530 eV. In Fig. 7, and subsequent figures the intensities are normalized to the *peak maximum*, so the Si-O intensity does not actually increase in absolute intensity. Relative to Si-O, most of the oxygen associated with cobalt is removed, as expected from the 90% reduction determined previously. In Fig. 7, the Si-O line narrows and

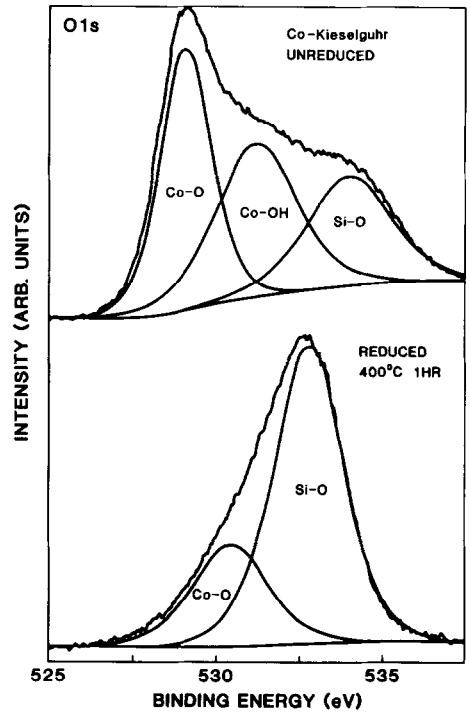

FIG. 7. Oxygen 1*s* spectra of unreduced and reduced Co–KG catalyst at 400°C including curve-fitting analysis (three-peak fit). Both the Co-O and Co-OH components are considerably attenuated after reduction, due to conversion of cobalt to the metallic phase. All peaks are normalized to the peak maximum so the change in Si-O intensity is only apparent. For most of the catalysts the Si-O intensity is a measure of the exposed KG surface and is approximately constant.

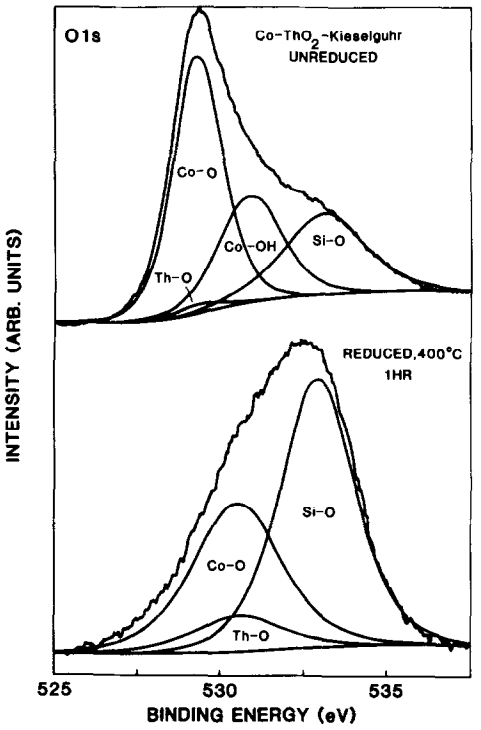

FIG. 8. Oxygen 1*s* spectra, including curve-fitted components (three-peak fit) of the Co-ThO_2–KG catalysts before and after reduction at 400°C. The Th-O contribution is calculated from the Th $4f_{7/2}$ intensity and included only to show its magnitude (since it has a similar binding energy to Co_3O_4 or CoO).

shifts to a somewhat lower B.E. after reduction and we attribute this to a decrease in the number of surface hydroxyl groups. For the thorium promoted case, we also observed a three-peak spectrum in Fig. 8 (unreduced), and after reduction only a two-peak fit is found with the Co-O line intensity dramatically reduced in intensity. The thorium component is small relative to the other lines. In both Figs. 7 and 8, therefore hydroxyl groups and oxygen associated with cobalt are lost after reduction, and the reduced spectra look similar, with only a small unreduced cobalt, or (cobalt + thorium) component. The fitting procedure for Figs. 7 and 8 indicated that the residual Co-O had a binding energy of ~530.5 eV. This increase from the initial Co_3O_4 value of 529.5 eV was observed previously in the spectra for Co_3O_4 reduction in Fig. 2, although only as high as 530 eV at low residual oxygen concentrations. We attribute this increase to a binding energy shift due to particle size changes during reduction. The higher residual binding energy for the unreduced Co-O on the supported catalysts must be due to decreased extraatomic relaxation which tends to increase binding energies and is of larger effect for species in contact with nonconducting surfaces.

Different results were obtained for the singly and doubly-promoted magnesia catalysts in Figs. 9 and 10. For Co-MgO–KG, a three-peak fit is obtained in the unreduced case (Fig. 9) with distinct Co-O, Mg-OH, and Si-O components. Although Co-OH overlapped with Mg-OH, both the O 1*s* intensity calculated from the Mg 1*s* signal and

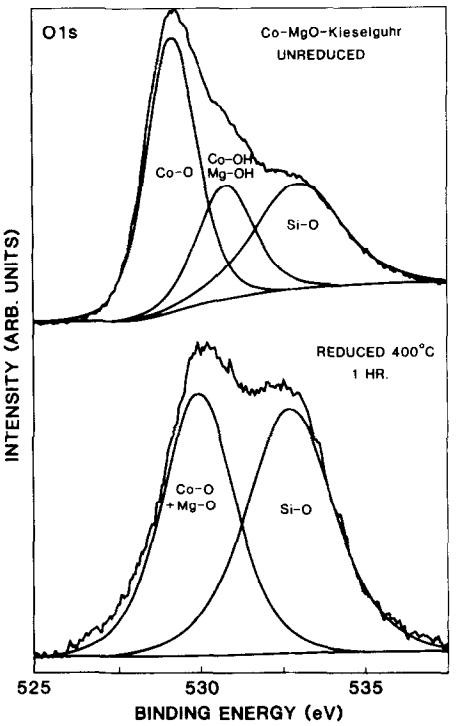

FIG. 9. Oxygen 1*s* spectra including curve-fitted components for the Co-MgO–KG catalysts before and after reduction at 400°C. After reduction the Co-O and Mg-OH lines shift to form a new peak at 530.0 ± 0.2 eV. We attribute this to solid solution formation between CoO and MgO. The calculated Mg-OH intensity from the Mg 1*s* line indicates only a small cobalt-hydroxyl contribution to this line.

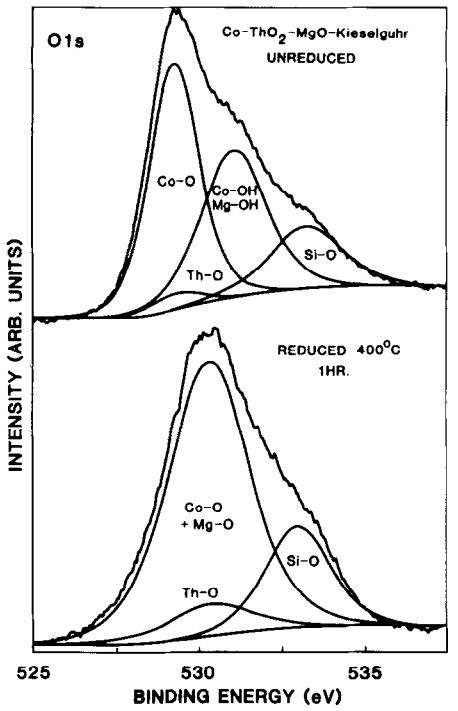

FIG. 10. Oxygen 1*s* spectra including curve-fitted components for the Co-ThO_2-MgO-KG catalyst before and after reduction at 400°C. After reduction the Co-O and Mg-OH lines shift to form a new peak attributed to solid solution formation between CoO and MgO. The Th-O peak is shown only to indicate its magnitude (as calculated from Th $4f_{7/2}$), and it is not known whether this component participates in the solid solution formation.

the observation of highly hydroxylated Mg-O components in all the reference phases ruled out any substantial Co-OH component in this case. After reduction, an O 1*s* doublet was observed, and only two peaks could be fitted to the spectrum. The large unreduced component, at ~530 eV is similar to both CoO (529.6 eV) and MgO (530.0 eV) O 1*s* positions and of considerable magnitude relative to silicon-oxygen. A similar effect was observed for the fully promoted Co-ThO_2-MgO-KG catalyst in Fig. 10. In the calcined state, three resolved Co-O, Mg-OH, and Si-O lines are fitted (with a small Th-O peak) with minimal cobalt-hydroxyl contribution to the Mg-OH line but after reduction a new single line is found at 530.0 ± 0.2 eV. This binding energy is similar to both CoO and MgO within 0.3 eV, and based on this value must contain minimal hydroxyl contributions from either Co-OH or Mg-OH species. The relative intensities of the (Co-O + Mg-O) and (Si-O) lines after reduction are different in Figs. 9 and 10. This is not an artifact of the fitting procedure, but may be a consequence of the different distributions of the two components.

In summary, the O 1*s* spectra for the four catalysts studied show considerably more reduction for the non-magnesia-containing catalysts at 400°C. Whereas the Co_3O_4 and MgO lines have B.E. positions similar to the oxide and hydroxide, respectively, in the calcined catalyst, after reduction the irreducible cobalt-oxygen component and magnesia lines form a single broader peak which can be assigned to both CoO and MgO (~530–530.2 eV). In addition, surface hydroxylation which is observed for both the Si-O Co-OH, and Mg-OH components on some of the calcined catalysts, disappears after reduction. Our calculations confirm that the unreduced oxygen component in the magnesia-containing catalysts must contain both cobalt and magnesium contributions, with the cobalt being present as Co(II) as determined from the Co 2*p* spectra.

3.4. Catalyst Structure and XPS Line Intensities

In order to further characterize the calcined and reduced catalysts, we measured quantitative peak area ratios (intensities) for Co $2p_{3/2}$, Mg 1*s*, and Th $4f_{7/2}$ relative to the Si 2*s* line of the Kieselguhr support. The results are shown in Table 4. As an essential correlation with this data, we also show transmission electron micrographs of several of the catalysts in Fig. 11. The interpretation of the XPS intensities is critically dependent on the model which is adopted to describe the distribution of the various phases. Since the original Kieselguhr BET surface area is ~4 m^2/g with the calcined catalysts ranging from 60

TABLE 4

Experimental Intensity Ratios[a] for Metal and Promoter Lines Relative to Si 2*s* Compared with Theory, before and after Reduction at 400°C for 1 h

Catalyst	Co $2p_{3/2}$/Si 2*s*	Mg 1*s*/Si 2*s*	Th $4f_{7/2}$/Si 2*s*
Co-ThO_2-MgO-Kg			
Unreduced	53.2	28.9	5.1
Reduced	58.8	24.7	4.5
Co-MgO-KG			
Unreduced	37.4	18.9	—
Reduced	34.7	25.1	—
Co-ThO_2-KG			
Unreduced	34.9	—	2.2
Reduced	17.4	—	2.5
Co-SiO_2			
Unreduced	30.6	—	—
Reduced	16.1	—	—
Theory[b] (Homogeneous dispersion)	6.7	1.6	0.2
Theory[c] (Monolayer deposition on 4 m^2/g support)	353	162	9.0

[a] Integral area ratios with a linear background.

[b] Assuming a homogeneous solid solution of all components, and no attenuation of the silica support.

[c] Calculated according to the work of Kerkhof and Moujlin (Ref. (*16*)) based on a Kieselguhr BET surface area of 4 m^2/g, and assuming monolayer deposition with no allowance for particle growth.

to 100 m^2/g, any attempt to calculate metal-to-silicon ratios based on a uniform deposition model will obviously be incorrect.

In Fig. 11a, both the Kieselguhr matrix and physically detached clumps of Co_3O_4 and the other oxides can be seen. A general examination of these catalysts under low power showed that much of the cobalt oxide is not attached to the Kieselguhr at all, although most of the Kieselguhr is partially covered in an irregular manner with small Co_3O_4 particles. In Fig. 11b, the nature of these particles can be seen; small crystalline particles, roughly spherical and approximately 5–10 nm in diameter, attached to one another in a network of "chains." Diffraction patterns of promoted and unpromoted catalysts gave similar results, showing only a Co_3O_4 pattern, with the MgO and ThO_2 too faint to be detected. Results for a reduced (400°C, 1 h) and passivated Co–KG catalyst after transfer through air are shown in Fig. 11c. The passivation procedure (slow oxidation to form a light skin of oxide) appears to have been successful since diffraction patterns of the particles revealed both fcc and hcp forms of metallic cobalt together with some CoO. Of particular interest is the change in morphology in Fig. 11c relative to the precursor oxides; whereas many smaller particles are intact, others have fused together to form larger agglomerated particles (up to 20–30 nm in size). Apart from this agglomeration of metallic cobalt, the general distribution of cobalt attached to Kieselguhr and unattached cobalt clumps was similar to the calcined precursors, for all the catalysts.

In Table 4, the intensity ratios can be compared with calculated ratios based on two models: (a) a homogeneous distribution of all oxides within the particles, with no attenuation of the silica support and (b) monolayer deposition of all the oxide on the support, based on Kerkhof and Moujlin's (*16*) calculation. The latter model gives grossly overestimated ratios, in agreement with the electron micrographs which show physical separation and only partial coverage of the Kieselguhr by promoted oxide. The first model gives ratios which are generally too low, which indicates that coverage of the Kieselguhr by some of the particles has occurred, as seen in Fig. 11, with consequent attenuation of the silicon 2*s* line (although this effect could be partly caused by the larger particle size of the Kieselguhr). Since the cobalt particle coverage on the Kieselguhr is nonuniform we cannot estimate exactly what the attenuation of the Si 2*s* will be, but the difference of a factor of 8–9 in the cobalt intensity between theory and experiment in Table 4 suggests it is substantial. Of more interest, however, are the relative Co : Mg : Th ratios. Since the oxides form an essentially independent phase, i.e., 5- to 10-nm particles, their surface composition should be similar to the theoretical ratio predicted from the homogeneous dispersion calculation in Table 4. The results in Table 4 show on enhancement of Mg and Th in the surface compositions by up to a factor of 2–3

over the expected values. Since oxide particle size variations are not large this must be attributed to an inhomogeneous distribution of Mg and Th, with a segregation occurring in the outer layers of the particles, perhaps as a result of nonuniform composition dur-

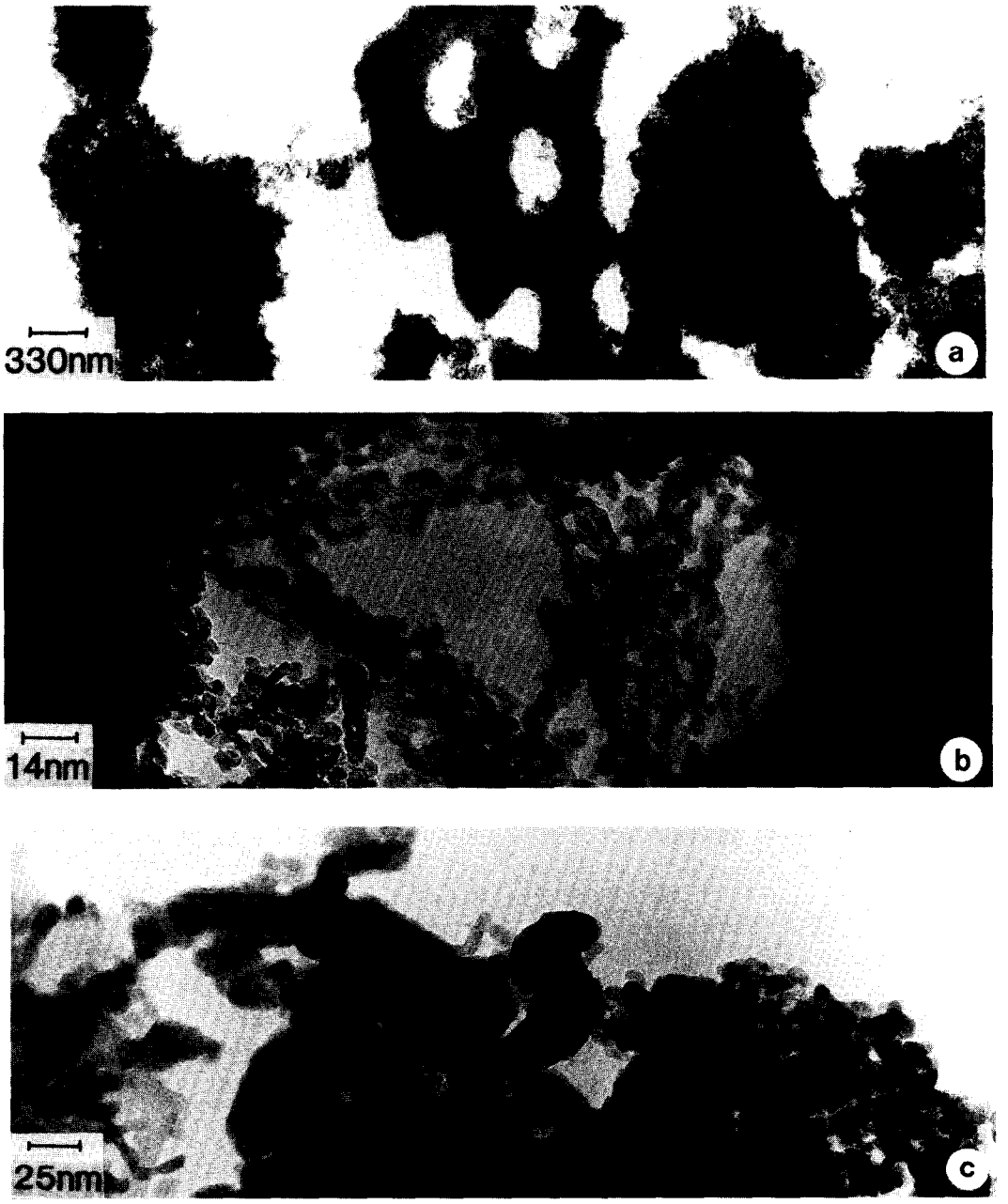

FIG. 11. Transmission electron micrographs of (a) unreduced Co–KG catalyst showing precipitation of Co_3O_4 on the KG and in unrelated aggregates. (b) Higher magnification micrograph showing fully promoted Co-ThO_2-MgO–KG particles (~5–10 nm); agglomerated in a Kieselguhr pore. (c) Reduced (400°C) and passivated Co–KG catalyst showing metallic cobalt, apparently sintered by fusion of adjacent particles. Due to air exposure of the reduced catalysts, most of the smaller particles were completely reoxidized and only larger passivated metal particles can be observed.

ing precipitation. After reduction, these relative ratios do not change dramatically. On unpromoted and Th-promoted Co–KG, a decrease in the Co/Si ratio is observed after reduction by almost a factor of 2, with smaller changes occurring for the MgO-promoted catalysts. This is attributed to sintering and fusion of the metallic cobalt particles on the more highly reducible catalysts, which lowers the cobalt signal (since more cobalt has become inaccessible to the 30-Å analysis depth of the XPS probe). In summary, the XPS results show an inhomogeneous distribution of the promoters Mg and Th relative to cobalt, and evidence for sintering of cobalt after reduction. Electron microscopy establishes the reason for the large change in surface area from support to calcined catalyst, and provides evidence for physical separation of much of the cobalt and the Kieselguhr, with observation of cobalt metal particle fusion after reduction of the highly reducible catalysts.

4. DISCUSSION

Based on the previous results, we propose a model for the reduction of the promoted Co/Kieselguhr catalysts and the effects of the promoters on this process. In the calcined state, Co_3O_4 is the dominant cobalt component on all catalysts, although substantial surface hydroxylation of this phase was present on Co–KG and Co-ThO_2–KG. The presence of surface hydroxyl groups was deduced primarly from the appearance of a third peak near 531.0 eV in the O 1*s* spectra of the Co–KG and Co-ThO_2–KG catalysts. On the magnesia-containing catalysts, cobalt was present as Co_3O_4 with the magnesium surface component highly hydroxylated and present in a higher concentration than expected from the bulk loading. This surface segregation of magnesium may explain why we observed lower Co-OH components on the magnesia-promoted catalysts compared with the non-magnesia cases. It is possible that variations in surface hydroxylation between the particles attached to the Kieselguhr and the detached particles may also have occurred. Whatever the nature of the surface hydroxyls observed, whether they be due to $Co(OH)_2$, or $Mg(OH)_2$ or mixed Co,Mg,O_x,OH_y phases, these groups disappeared after reduction and did not appear to play an important role in the reduction. This is supported by the low-temperature (<300°C) reduction of bulk $Co(OH)_2$ observed previously. The promoters ThO_2 and MgO appear *not* to have reacted with Co_3O_4 or the silica in the calcined state since similar reduction profiles were observed in the TPR for the first, low-temperature peak in all catalysts studied. The first phase of reduction occurs when Co_3O_4 is reduced to CoO:

$$Co_3O_4 + H_2 \rightarrow 3CoO + H_2O \quad (1)$$

Each catalyst displayed a single peak below 300°C in the TPR with an area of 25% ± 3 of the total reduction, consistent with the above process. $Co(OH)_2$ also reduced rapidly at 300°C and this explains the loss of the hydroxyl contribution in the O 1*s* spectra of Figs. 7 and 8 after reduction. Once CoO is formed, there are two possible pathways:

$$CoO + H_2 \rightarrow Co + H_2O \quad (2)$$

$$CoO + MgO \rightarrow (Co, Mg)O \text{ (solid solution)}$$

$$CoO + ThO_2 \rightarrow (Co, Th)O \text{ (unknown phase)} \quad (3)$$

Reduction of CoO to the metal occurs in the second TPR peak of Co_3O_4 and is slow at 300°C (1–2 h) but rapid at 400°C (<1 h). For the magnesia-containing catalysts we propose that CoO, once formed under reducing conditions can form a *solid solution* with MgO at 400°C and this new phase is more resistant to reduction. The TPR results of Fig. 4 showed a peak maximum near 500–600°C for this phase. These results indicated a higher reduction temperature for CoO in association with thoria (Fig. 4), similar to the MgO-promoted cases. The reac-

tion with thorium oxide must also occur, but was not spectroscopically observable. Prediction of the static reduction results from the TPR is difficult since small differences in the reduction *rate* at 400°C can produce large differences in the *total* reduction after 1 h. We observed previously that the actual reduction *rates* for the Co–KG and Co-ThO_2–KG catalysts at 400°C were higher than the MgO-containing ones, despite the peak maximum temperature being similar for the thoria-promoted case (500–600°C).

The formation of CoO-MgO solid solutions is well known and has been studied by many techniques, including XPS (*9*). The system is homogeneous without any major segregation of either component. Preparation is normally carried out by heating cobalt nitrate-impregnated MgO to 1200°C because Co_3O_4 is unstable at these temperatures in air (*9*). We attempted several preparations of these CoO-MgO solid solutions by the high temperature method but were unsuccessful due to loss of MgO from the preparation by sublimation. The literature data on XPS analyses of CoO-MgO (9) is vague on the question of air sensitivity and we suspect that surface oxidation is probably significant, as it is for CoO. One point of agreement is the similarity of our (Co, Mg-O) O 1*s* binding energy (530.0 ± 0.5 eV) with that measured by Cimino *et al.* (*9*) (530.0 eV) for the solid solutions. One cannot prove that a solid solution is formed from this value alone, however, and we have to rely on the implications of the reduction behavior of this phase to make a case for solid solution formation. We also prepared Co_3O_4-MgO mixtures by the same coprecipitation method as the catalysts and obtained similar TPR results and XPS line shifts to the supported catalysts. In particular the XPS results showed two components prior to reduction forming a single O 1*s* line near 530.0 eV with limited reduction at 400°C. Examination of the reduced Co_3O_4-MgO mixture with XRD after air exposure showed only traces of possible solid solution lines, but oxidation of these samples had definitely occurred (no anaerobic XRD cell was available). We therefore have strong, but not conclusive evidence for solid solution formation between CoO and MgO in these catalysts. Our results show clearly that CoO *must be formed* in order for the reaction to take place because no reaction of Co_3O_4 with MgO was observed after the 350°C calcination in air via XPS. CoO can only be formed by reducing Co_3O_4 in H_2, and it appears that a temperature as low as 400°C is sufficient to activate solid solution formation. The Kieselguhr support does not affect the process, since identical TPR and XPS results were obtained on coprecipitated Co_3O_4-MgO mixtures. The nature of the ThO_2-CoO interaction is less clear, since they have dissimilar crystal structures. Since ThO_2 has the fluorite structure whereas CoO has the rock-salt structure, solid solutions are not possible. TPR results show considerable interaction between the two however, similar to the MgO-promoted cases. We postulate that a mixed ThO_2-CoO phase of unknown structure is formed which has a higher kinetic or thermodynamic barrier to reduction.

Interaction of Co(II) ions with other solid-state phases has been observed on catalysts with XPS in several other systems (*3, 5, 7*). Chin and Hercules (*5*) found a variation in the reducibility of Co/Al_2O_3 catalysts and attributed the results to reaction of Co(II) with the Al_2O_3 support to form octahedrally or tetrahedrally coordinated cobalt at the surface. Similar results were obtained by Declerck-Grimee *et al.* (*7*). Castner (*3*) investigated the reducibility of cobalt on SiO_2, TiO_2, and Al_2O_3 and found evidence for surface interactions on TiO_2 and Al_2O_3. Co_3O_4 and Co/SiO_2 were found to reduce almost quantitatively to the metal at 400°C, with little evidence for metal–support interactions (*3*).

Our results support the very early ideas by Anderson and others that there is a substantial interaction between ThO_2, MgO, and cobalt oxide in the activation of Fis-

cher–Tropsch catalysts. We have shown, in addition, that the reaction occurs only when the reactive CoO phase is generated by reduction, and that the support Kieselguhr does not affect the process. Promoted cobalt catalysts have a more controllable degree of reduction to the metal because the reduction of the CoO-promoter phase is spread over a wider temperature range than the unpromoted catalysts. The initial reduction of Co_3O_4 to CoO has a different activation energy, however, and is complete within a few minutes at 300°C on all catalysts.

Whereas Kieselguhr is an inherent component in all of the catalysts studied, both TPR and TEM measurements indicate that it acts as little more than a volume enhancer rather than a support in the present work. Since it is added after the coprecipitation has started it is not surprising that much of the agglomeration of particles proceeds independently of the "support." Since much of the reduction and cobalt particle formation proceeds independently of the Kieselguhr, the role of the unreduced CoO-MgO solid solution and other phases may be to prevent the fusion and sintering of the metallic cobalt, by acting as a "support." The importance of new phases or solid solutions involving cobalt in Fischer–Tropsch catalysts has been highlighted in recent work by Lapidus (*17, 18*). Surface compounds involving MgO and V_2O_5 have been detected using ESR, IR, and TPR, but the compound could not be identified with XRD (*19*).

5. CONCLUSIONS

It is evident from our study that there is a strong interaction of the promoters MgO and ThO_2 with CoO. Particularly in the case of magnesia, CoO forms what appears to be a solid-solution phase, identified with XPS, which is more resistant to reduction. Thorium oxide has the same effect but is more difficult to confirm spectroscopically due to coincidental O 1*s* lines for ThO_2 and CoO and the lower loading. Co_3O_4, present initially on all catalysts as ~5- to 10-nm particles reduces rapidly to CoO at $T > 250$°C. The rate of reduction to the metal at higher temperatures (~400°C) is limited by the type of phase present. On unpromoted catalysts CoO reduces to the metal, whereas on promoted catalysts the CoO-promoter phases have higher activation energies for reduction.

The inhibition of cobalt reduction by promoters enables more control over the percentage active metal at the surface and possibly its morphology on the catalyst, because of the broader reduction profile. In incompletely reduced catalysts, the new CoO-promoter phases will be present and further work is needed to identify their role in the Fischer–Tropsch synthesis.

ACKNOWLEDGMENT

The authors wish to thank Dr. J. V. Sanders for the electron micrographs of the catalysts in the present work.

REFERENCES

1. Emmett, P. H., Ed., "Catalysis," Vol. IV, Chap. 2. Reinhold, New York, 1956.
2. Anderson, R. B., *in* "Catalysis" (P. H. Emmett, Ed.), Vol. IV, Chap. 2, p. 82. Reinhold, New York, 1956.
3. Castner, D. G., and Santilli, D. S., *ACS Symp. Ser.* No. 248, 39 (1984).
4. Sato, K., Inoue, Y., Kojima, I., Miyazaki, E., and Yasumori, I., *J. Chem. Soc. Faraday Trans. I* **80,** 841 (1984).
5. Chin, R. L., and Hercules, D. M., *J. Phys. Chem.* **86,** 3079 (1982).
6. Chin, R. L., and Hercules, D. M., *J. Phys. Chem.* **86,** 360 (1982).
7. Declerck-Grimee, R. I., Canesson, P., Friedman, R. M., and Friplat, J. J., *J. Phys. Chem.* **82,** 885 (1978).
8. Chung, K. S., and Massoth, F. E., *J. Catal.* **64,** 320 (1980).
9. Cimino, A., DeAngelis, B. A., and Minelli, G., *Surf. Interface Anal.* **5,** 150 (1983).
10. U.S. Patent 4,088,671.
11. Scofield, J. H., *J. Electron Spectrosc. Relat. Phenom.* **8,** 129 (1976).
12. Ansell, R. O., Dickinson, T., Povey, A. F., and Sherwood, P. M. A., *J. Electroanal. Chem.* **98,** 79 (1979).

13. Proctor, A., and Sherwood, P. M. A., *J. Electron Spectrosc. Relat. Phenom.* **27,** 39 (1982).
14. Chuang, T. J., Brundle, C. R., and Rice, D. W., *Surf. Sci.* **59,** 413 (1976).
15. Brundle, C. R., Chuang, T. J., and Rice, D. W., *Surf. Sci.* **60,** 286 (1976).
16. Kerkhof, F. P. J. M., and Moujlin, J. A., *J. Phys. Chem.* **83,** 1612 (1979).
17. Lapidus, A. L., Hoang Chong Yem, and Krylova, A., *Neftekhimiya* **23,** 779 (1983).
18. Lapidus, A. L., *Izv. Akad. Nauk. SSSR, Ser. Khim.* (1), 60 (1984).
19. Iwamoto, M., Takenaka, T., Matsukami, K., Hirata, J., Kagawa, S., Izume, J., *Appl. Catal.* **16,** 153 (1985).